ISSN 1063-7729, Astronomy Reports, Vol. 51, No. 5, 2007, pp. 327–381. ©Pleiades Publishing, Ltd., 2007. Original Russian Text ©V.V. Bobylev, A.T. Bajkova, 2007, published in Astronomicheskiĭ Zhurnal, 2007, Vol. 84, No. 5, pp. 418–428.

Analysis of the Velocity Field of F and G Dwarfs in the Solar Neighborhood as a Function of Age

V. V. Bobylev and A. T. Bajkova

Pulkovo Astronomical Observatory, Russian Academy of Sciences, Pulkovskoe sh. 65, St.Petersburg, 196140 Russia

Received June 18, 2006; in final form, October 12, 2006

Abstract — The space velocities from the catalog of Nordström et al. (2004) are used to trace variations of a number of kinematic parameters of single F and G dwarfs as a function of their age. The vertex deviation of disk stars increases from $7 \pm 1^\circ$ to $15 \pm 2^\circ$ as the mean age decreases from 4.3 to 1.5 Gyr. The two-dimensional velocity distributions in the UV, UW, and VW planes are analyzed. The evolution of the main peaks in the velocity distributions can be followed to an average age of ≈ 9 Gyr. We find that: (1) in the distributions of the UV velocity components, stars of different types are concentrated toward several stable peaks (the Hyades, Pleiades, and Sirius Cluster), suggesting that the stars belonging to these formations did not form simultaneously; (2) the peak associated with the Hyades Cluster dominates in all age intervals; and (3) the Hyades peak is strongest for stars with an average age of 1.5 Gyr, suggesting that this peak contains a considerable fraction of stars from the Hyades cluster. The age dependences of the kinematic parameters exhibit a break near ≈ 4.5 Gyr, which can be explained as an effect of the different contributions of stars of the thin and thick disks. The Strömberg relation yields a solar LSR velocity of $V_{\odot LSR} = (8.7, 6.2, 7.2) \pm (0.5, 2.2, 0.8)$ km/s.

PACS numbers : 97.10.Wn, 97.20.Jg, 97.10.Cv, 98.35.Df, 98.35.Pr
DOI: 10.1134/S1063772907050034

1. INTRODUCTION

Analysis of the velocity field for stars in the solar neighborhood is of great importance for understanding the kinematics and evolution of various structural components of the Galaxy. As is now well known, the distribution of stellar space velocities has a complex small-scale structure, which could be due to various physical factors. Whereas the statistical method [1], which can yield such features of the distribution as the dispersion of the residual velocities and the orientation of the Schwarzschild ellipsoid, was previously sufficient to describe the observed velocity field, we must now use more subtle methods (spatially noninvariant (adaptive) smoothing, as that used by Skuljan et al. [2], wavelet analysis, etc.) to identify stable structural formations, e.g., in the form of peaks [2, 3] or branches [2].

The distributions of space velocities of stars in the solar neighborhood exhibit several characteristic peaks associated with well-known open clusters [2, 4.6], such as the Pleiades (with an age of 70. 125 Myr [7]), the Sirius cluster (500 Myr [8]), and the Hyades (650 Myr [9]). These are fairly young compared to the age of the Galaxy (of the order of 10 Gyr). Chandrasekhar [10] showed that the time scale for the stability of an open cluster is an order of magnitude shorter than the age of the Galaxy. This imposes constraints on using the theory of streaming motions [11.13]. It is therefore of great interest to study the kinematic characteristics of stars as a function of their age.

The high-precision parallaxes and proper motions provided for a large number of stars by the HIPPARCOS [14] catalog revealed fine structure in the distribution of space velocities for stars in the solar neighborhood [2, 3, 15]. However, these were only preliminary results, since they were either based on modelled radial velocities [3, 15] or used insufficiently accurate radial velocities [2]. In this connection, the survey of Nordström et al. [16] is clearly of great value, as it gives high-precision radial velocities, proper motions, and parallaxes for a large and homogeneous sample of F and G stars and, which is very important,

reliable estimates of the ages of individual stars.

The aim of the current paper is to study the structure of the distribution of space velocities of F and G dwarfs using the age estimates listed in [16] in order to follow the evolution of the main peaks associated with known clusters. Looking for concentrations of stars of different ages toward the same peaks is also very important because it would imply the action of some continuously operating gravitational factor (spiral density waves, a bar). In particular, Famaey et al. [17] independently argue for this possibility based on other methods applied to other stellar samples.

In this paper, we use the statistical method to determine the elements of the Schwarzschild ellipsoid, and apply an adaptive Gaussian smoothing method to the initial stellar distributions to analyze the fine structure of the velocity field.

We also aim to verify the Strömberg relation based on space velocities obtained through a joint analysis of proper motions from the HIPPARCOS catalog, high-precision radial velocities, and stellar age estimates.

2. INITIAL DATA

The catalog [16], which contains about 14 000 F and G dwarfs, gives original high-recision radial velocities (with typical errors of $\approx$ 0.25 km/s), previously published $uvby\beta$ photometry in the Strömgren system, HIPPARCOS parallaxes, supplemented in a number of cases by photometric distances, and stellar proper motions from the HIPPARCOS and TYCHO- 2 [18] catalogs. Most of the catalog stars have age estimates determined with typical accuracies of $< 50\%$. We considered only single stars located within 200 pc of the Sun. We did not consider double and multiple stars marked by a flag in column 4 of the table in [16].We used only stars with age estimates τ. We corrected the radial velocities and proper motions for Galactic rotation using the Oort constants $A = 13.7$ km/s·kpc and $B = -12.9$ km/s·kpc [19]. In the first part of this paper, we analyze the nearest single stars for which

$$e_\pi/\pi < 0.1, \quad e_\tau/\tau < 0.3. \tag{1}$$

These are stars with the best age and distance estimates. We need a large number of such stars to construct two-dimensional velocity-field distributions of suitable quality. To this end, we used slightly more distant single stars satisfying the conditions

$$\begin{gathered} e_\pi/\pi < 0.2, \\ e_\tau/\tau < 0.5, \\ |V_{pec}| < 100 \ \text{km/s}, \end{gathered} \tag{2}$$

where V_{pec} is the peculiar velocity of a star relative to the Local Standard of Rest (LSR). We adopted the solar velocity relative to the LSR presented by Dehnen and Binney [15]: $(X_\odot, Y_\odot, Z_\odot)_{\text{МСП}} = (10.00 \pm 0.36, 5.25 \pm 0.62, 7.17 \pm 0.38)$ km/s.

3. ANALYSIS METHODS

3.1. Statistical Method

We use here a Cartesian coordinate system with axes directed away from the observer and toward the Galactic center ($l = 0°, b = 0°$, the x axis), in the direction of Galactic rotation ($l = 90°, b = 0°$, the y axis), and toward the North Galactic Pole ($b = 90°$, the z axis).

We determined the elements of the Schwarzschild ellipsoid using the well-known statistical method described in detail in [1, 20–22]. We first determined the components of the Solar velocity by solving the Kovalsky.Arie equations, then determined the elements of the residual-velocity dispersion tensor from a least-squares solution to the system of equations in six unknowns. Analysis of the eigenvalues of the velocity-dispersion tensor yields the principal axes of the residual-velocity ellipsoid, which we denote $\sigma_{1,2,3}$, and the directions of the principal axes, which we denote $l_{1,2,3}, b_{1,2,3}$. We use the method of Parenago [23] with fourth-order moments to estimate the errors in the parameters $\sigma_{1,2,3}$.

3.2. Constructing the Two-Dimensional Stellar Velocity Distributions

We estimated the two-dimensional probability density $f(U,V)$ based on the computed, discrete UV velocity components using an adaptive-smoothing method. Unlike Skuljan et al. [2], we used the radially-symmetric Gaussian kernel

$$K(r) = \frac{1}{\sqrt{2\pi}\sigma} \exp -\frac{r^2}{\sigma^2},$$

where $r^2 = x^2 + y^2$. This function obeys the condition $\int K(r)dr = 1$, which is necessary for estimating the probability density. The typical uncertainties in the velocities in our case is 2 km/s, which, among other factors, determined our choice of discretization interval for the two-dimensional maps; the area of each square pixel is $s = 2 \times 2\text{km}^2/\text{s}^2$.

The main idea of the method consists in the following. At each point, we smooth with a beam whose size is determined by σ and varies in accordance with the data density in the neighborhood of the point considered. Thus, the smoothing is performed with a relatively narrow beam in regions with high data densities, with the beam width increasing as the data density decreases.

We used the following form of adaptive smoothing at an arbitrary point $\xi = (U,V)$ [2]:

$$\hat{f}(\xi) = \frac{1}{n}\sum_{i=1}^{n} K\left(\frac{\xi - \xi_i}{h\lambda_i}\right),$$

where $\xi_i = (U_i, V_i)$, λ_i is the local dimensionless beam parameter at ξ_i, h is a general smoothing parameter, and n is the number of data points $\xi_i = (U_i, V_i)$. The parameter λ_i of the two-dimensional plane UV is determined at each point as follows:

$$\lambda_i = \sqrt{\frac{g}{\hat{f}(\xi)}}\,, \qquad \ln g = \frac{1}{n}\sum_{i=1}^{n} \ln \hat{f}(\xi),$$

where g is the geometric mean of $\hat{f}(\xi)$.

It is obvious that, to determine λ_i, we must know the distribution $\hat{f}(\xi)$, which, in turn, can be determined if all the λ_i are known. Therefore, the sought for distribution must be reconstructed iteratively. As a first approximation, we used the distribution obtained by smoothing the initial UV map using a fixed-sized beam. We found the best-fit value of h by minimizing the mean squared residual for the difference between the estimated distribution $\hat{f}(\xi)$ and true distribution $f(\xi)$, which was equal to about 9 km/s in our case.

4. RESULTS AND DISCUSSION

4.1. Asymmetric Drift

Figures 1 and 2 show the group velocities of stars (with reversed sign) as functions of the square of the residual-velocity dispersion S^2 and of the stellar age τ. Like Dehnen and Binney [15], we derived the dependences in Fig.1 using the quantity $S^2 = 1.14{\cdot}\sigma_{xx}^2$. The horizontal bars in Fig. 1 show the one-sigma uncertainties in S^2, and the similar bars in Fig. 2 show the boundaries of the age intervals corresponding to the mean error of the stellar age determination.

The dependence

$$Y_\odot = a \cdot S^2 + b, \tag{3}$$

shown in the middle plot in Fig. 1 (the Strömberg relation) has the parameters $a = 0.0122 \pm 0.0019$ (km/s)$^{-1}$ and $b = 6.2 \pm 2.2$ km/s. We obtained these values using all the available data.

Extrapolating to zero velocity dispersion yields for the LSR velocity of the Sun $Y_{\odot\ \mathrm{MCП}} = 6.2 \pm 2.2$ km/s. The relatively large error of this velocity is due (middle plot in Fig. 1) to the substantial scatter in the data points near $S^2 = 1000$. As is also evident from the middle plot in Fig. 2, out to an age of $\tau = 4 - 5$ Gyr, virtually all the points $Y_\odot$ are almost parallel to the horizontal axis, and the dependence shows a peculiar kink at $\tau = 4 - 5$ Gyr. Figure 4 from Dehnen and Binney [15], which exhibits a depressed portion of the V dependence for velocity dispersions $S^2 \approx 300 - 700$(km/s)2, shows a similar pattern, as does Fig. 6 from Olling and Dehnen [24] in the color index interval $(B-V)_\circ \approx 0 - 0.3$. After dropping two data points $Y_\odot$in Fig. 1 that correspond to ages of $\tau = 3.7$ and 5.1 Gyr, i.e., to the depressed portion of the plot, we obtained for the unknown parameters $a = 0.0125 \pm 0.0009$ (km/s)$^{-1}$ and $Y_{\odot\ \mathrm{MCП}} = 7.1 \pm 1.1$ km/s; the accuracy is now twice as good as in the previous case.

We thus conclude that the effect of this feature is significant and not accidental. It may be that the form of model relation (3) used to describe the actual kinematics of stars must be more complex, since this feature is difficult to explain as an effect of random errors in the stellar ages. Alternatively, we may observe a discontinuity due to stars belonging to the thick or thin disk. We discuss this possibility below in Section 3.3. Overall, our a and $Y_\odot$ values agree with the results of Dehnen and Binney [15], who obtained the estimates $a = 0.0125$ (km/s)$^{-1}$ and $Y_{\odot\ \mathrm{LSR}} = 5.25 \pm 0.62$ km/s, based on the proper motions of a much greater number of stars.

We calculated the other two components of the solar velocity by averaging the velocities of seven stars, without the youngest stars: $X_{\odot\mathrm{LSR}} = 8.7{\pm}0.5$ km/s and $Z_{\odot\mathrm{LSR}} = 7.2 \pm 0.8$ km/s. The corresponding means in Fig. 1 are indicated by dashed lines.

Equation (3) can be written $Y_\odot = V_\varphi + Y_{\odot\ \mathrm{LSR}}$, where V_φ is the average velocity lag of stars with respect to the circular velocity of Galactic rotation at the distance of the Sun from the Galactic center (R_o= 8 kpc), i.e., the asymmetric drift velocity. To get some idea of the expected dependence $Y_\odot$ on time, we can substitute the parameters derived from $\sigma = c \cdot \tau^\gamma$ into (3), where $\sigma \equiv S$. We find that the expected dependence has the form of a power-law function with index $\gamma = 0.66$. We derived the dependence shown by the dashed line in the middle plot in Fig. 2 directly from the initial data; its index is $\gamma = 0.41 \pm 0.10$. If we drop the two data points corresponding to ages $\tau = 3.7$ and 5.1 Gyr, we obtain the index $\gamma = 0.37 \pm 0.06$.

The theory of the dynamic evolution of the Galaxy [25] assumes that the dependence V_φ obeys the relation

$$V_\varphi = \frac{\sigma_U^2}{2V_{\circ\ \mathrm{LSR}}}\left\{\frac{R}{\rho}\frac{d\rho}{dR} + 2\times\frac{R}{\sigma_U}\frac{d\sigma_U}{dR} + \left(1 - \frac{\sigma_V^2}{\sigma_U^2}\right) + \left(1 - \frac{\sigma_W^2}{\sigma_U^2}\right)\right\}, \tag{4}$$

where $d\rho/dR$ is the stellar-density gradient, R is Galactocentric distance, and $V_{\circ\ \mathrm{LSR}}$ is the rotation velocity of the local standard of rest.

The solid line and circles in Fig. 2 show the asymmetric drift velocity for disk stars. We drew this curve based on the results of Robin et al [26], which they obtained using formula (4) together with modern data on the distribution of stellar masses in the solar neighborhood and estimates of the velocity dispersions of HIPPARCOS stars as a function of age [27]. We

also used the parameter values [26] $V_{\circ\ \mathrm{LSR}} = 226$ km/s, $Y_{\odot\ \mathrm{LSR}} = 6.3$ km/s (we merged the age intervals 5.7 and 7.10 Gyr from Table 4 of Robin et al. [26] into a single interval). As is clear from Fig. 2, the dotted and solid lines, obtained using the different methods, are in good agreement.

4.2. Analysis of Two-Dimensional Velocity Distributions as a Function of Age

To construct the velocity distributions in the UV , UW, and VW planes, we used single stars meeting criteria (2). Unlike the previous case, the number of stars is 4880, and we subdivided them into four age groups containing approximately equal number of stars, which we refer to as t1–t4.

Figures 3.5 show the maps of the UV, UW, and VW velocity distributions for the age samples indicated above.We constructed all these maps using the adaptive smoothing algorithm (see Section 2.2). The lowest contour level and contour increment are 10% of the peak value in all figures. Tables 1 and 2 list the main kinematic parameters of the samples considered. Table 3 lists the relative values of the main peaks found in the maps. The coordinates of these peaks relative to the LSR are equal to (in km/s)$U = 20$, $V = 8$ for the Sirius peak; $U = 0$, $V = -2$ for the Coma peak; $U = -5$, $V = -16$ for the Pleiades peak; and $U = -26$, $V = -12$ for the Hyades peak.

As is clear from Table 1, the behavior of the variation of $Y_{\odot}$ for the samples t1–t4 exactly matches that shown in Fig. 1: the $Y_{\odot}$ values barely increase out to an age of $\tau = 4.3$ Gyr, and are equal to about 15 km/s. The speed $V_{\odot}$ also remains constant and equal to about 19 km/s.

As is evident from Table 2, the third axis b_3 does not deviate significantly from the direction toward the Galactic pole; the vertex deviation l_1 increases from $7 \pm 1^{\circ}$ for old stars to $15 \pm 2^{\circ}$ for stars with a mean age of 1.5 Gyr. This result agrees well with the conclusions of Dehnen and Binney [15], who found the vertex deviation for main-sequence HIPPARCOS stars as a function of color index.

The random errors in the stellar radial velocities decrease from ≈ 2 km/s for the youngest stars to ≈ 0.25 km/s for old stars. Therefore, the most reliable maps are those for the samples t2–t3, since, other conditions being the same, they have lower random space-velocity errors. Our Monte-Carlo numerical simulations showed that random errors in the stellar space velocities of 2 km/s shift the maxima of the UV velocity distributions by no more than $3 \div 4$ km/s, indicating the stability of the derived coordinates of the peaks.

It is clear from Figs. 3–5 and Table 3 that concentrations of stars in the form of stable peaks show up mostly in the distribution of the UV velocity components (Fig. 3). The Hyades peak dominates in all age intervals. The relative intensity of the Hyades peak ($U = -26$ km/s) for young stars is so high that we had to exclude the youngest stars when determining the solar-velocity vector relative to the LSR (see the dependences for $X_{\odot}$ in Figs. 1.2). This leads us to conclude that the kinematics of the youngest stars is determined by their membership in the Hyades peak.

We found no significant variations of the coordinates of the main peaks as a function of stellar age in samples t1–t4. Table 3 shows the variations of the relative intensities of the peaks.

It is evident from Fig. 3 that the orientations (vertex deviations) of individual isolated peaks, e.g., of the Hyades peak, vary appreciably as a function of the sample age. At the same time, the Hyades and Pleiades peaks form a branch-shaped extended structure whose orientation remains unchanged. See Skuljan et al. [2] for a detailed description of such structures in the UV-velocity distribution for a large number of HIPPARCOS stars.

Figure 3 also demonstrates the development of a structural feature centered on $U = -25$ and $V = -40$ km/s, which is usually associated with the ζ stream. The core of this feature shows up in all the samples, but it is branch-shaped only for sample t4, i.e., in the velocity distribution for the oldest stars.

Numerical simulations of disk heating by spiral waves carried out De Simone et al. [28] showed that the division of the UV distribution into branches and peaks can be explained by irregularities in the Galactic potential, but not by irregularities in the star formation processes. The effect of the bar on the evolution of the velocity ellipsoid and the distribution of residual stellar velocities are now topics of extensive studies [29, 30]. Babusiaux and Gilmore [31] provide strong arguments supporting the presence of a bar, based on an analysis of infrared observations of stars. Fux [29] showed that a bar in the Galactic center should result in the development of arms, and the Hercules arm is believed to be due to the effect of the bar [17, 32, 33].

Analysis of the UW distribution for sample t1 in Fig. 4 shows that the Hyades peak shows up conspicuously, along with the central peak. In the case of sample t4, which contains the oldest stars, the Hyades peak shows up as a prominent, isolated clump.

The VW velocity distributions (Fig. 5) for samples t1.t4 are fairly symmetric and regular. The oldest stars (t4) show a well-defined velocity lag and the ellipse-truncation effect.

On the whole, we conclude that stars of very different ages are concentrated toward several peaks associated with known open clusters. Our results agree with the conclusions of Famaey et al. [17], who selected samples of M and K giants belonging to individual peaks in the UV velocity plane and computed the isochrone ages of individual stars. They found that peaks contained stars covering very wide age intervals, suggesting that stars belonging to individual peaks did not form simultaneously. This is also the main conclusion of our paper.

4.3. Stars of the Thin and Thick Disks

The samples t1–t4 contain stars of both the thin and thick disk, and may also be slightly contaminated by halo stars. In this section, we subdivide stars in samples t1–t4 into thin-disk and thick-disk stars based on kinematic criteria, and analyze the age dependences of the group velocities of these stars. According to modern concepts, the conditions $|V_{pec}|$ <100 km/s and [Fe/H]>−0.5 dex separate out halo stars rather efficiently [34, 35].We selected a group of single stars meeting the criteria

$$e_\pi/\pi < 0.2, \quad e_\tau/\tau < 0.5,$$
$$|V_{pec}| < 60 \text{ км/с}, \quad [Fe/H] > -0.5 \text{ dex},$$

which we consider to be thin-disk stars. The second group, which contains mostly thick-disk stars, satisfies the conditions

$$e_\pi/\pi < 0.2, \quad e_\tau/\tau < 0.5,$$
$$60 \text{ км/с} < |V_{pec}| < 100 \text{ км/с},$$
$$[Fe/H] > -0.5 \text{ dex}.$$

The calculated kinematic parameters are listed in Table 1, where the thin-disk and thick-disk samples are indicated by a single and double prime, respectively; we calculated V_{pec} relative to the Sun. We show the age dependences of the resulting solar-velocity components in Fig. 6. Analysis of Table 1 and Fig. 6 shows that the $Z_\odot$ component shows the smallest differences between the two groups. The $X_\odot$ velocity component shows the greatest difference, which reaches 35 km/s for the youngest stars.

We found the velocity lags at an age of about 9 Gyr to be V_ϕ=11 km/s for thin-disk stars, reaching V_ϕ=35 km/s for thick-disk stars. These values are consistent with those currently taken to be the known kinematic characteristics of the thin and thick disks [24, 26].

It is obviously impossible to separate the evolution of stars of the thick and thin disks. However, as is clear from Table 1, the number of thick-disk stars increases appreciably with the sample age, resulting in the observed discontinuities in the dependences of $Y_\odot$ on τ and on S^2. This bend in the dependences of the kinematic parameters near ≈ 4 Gyr (Fig. 1, 2) can be explained by changes in the contributions of the thin-disk and thick-disk stars with stellar age.

It is evident from the middle part of Table 1 and the upper plot in Fig. 6 that $X_\odot$ for disk stars does not remain constant, i.e., there is a significant velocity gradient as a function of time, with this velocity reaching 3.0 ± 0.8 km/s for sample t4′ (or, in terms of signed quantities, $\overline{U} = -3.0 \pm 0.8$ km/s).We particularly point out this result, because, so far, only two large catalogs of high-precision stellar radial velocities measured with CORAVEL spectrometers are available: those of Nordström et al. [16] and Famey et al. [17] for dwarf and giant stars, respectively. In their analysis of high-precision space velocities of K and M giants in a sample of stars without high-velocity objects, Famey et al. [17] found $\overline{U} = -2.78 \pm 1.07$ km/s. This shows that an appreciable fraction of stars in the solar neighborhood may have systematic motions in the radial direction (along the Galactic radius vector), and also further complicates the problem of selecting stellar samples for the most rigorous determinations of the parameters of the local solar motion relative to the LSR.

CONCLUSIONS

We have used high-precision space velocities (with an average error of 2 km/s) for single F and G dwarfs within 200 pc of the Sun taken from the survey of Nordström et al. [16] to analyze the variation of the kinematic parameters of stars as a function of their age.

We find that the vertex deviation for disk stars increases from $7 \pm 1^\circ$ to $15 \pm 2^\circ$ as the mean age decreases from 4.3 to 1.5 Gyr.

We analyzed the main peaks in the two-dimensional stellar space velocity distributions in the UV, UW, and VW planes associated with known clusters, to determine how these peaks evolve with increasing age of the stellar sample, up to a limiting mean age of ≈ 9 Gyr. This analysis shows the following.

(1) In the UV-velocity distribution, stars with different ages are concentrated toward several stable peaks (the Hyades, Pleiades, and Sirius clusters). This indicates that stars belonging to these individual peaks did not all form simultaneously. This is the main conclusion of this work.

(2) The peak associated with Hyades cluster is the most conspicuous in all the age intervals.

(3) The Hyades peak is most prominent for stars with a mean age of 1.5 Gyr, suggesting that this peak contains a large fraction of Hyades cluster stars.

We show that the bend in the age dependences of the kinematic parameters near $\approx 4 - 5$ Gyr can be explained as an effect of the changing contributions of thin-disk and thick-disk stars. When redetermining the parameters of the asymmetric drift and the Strömberg relation, we found the dependence of $Y_\odot$ on the mean stellar age τ to show a discontinuity at $\tau \approx 5.1$ Gyr, with $Y_\odot$ remaining approximately constant at lower ages ($\approx$ 15 km/s). Removing outliers enabled us to increase the accuracy of the parameters of the Strömberg relation by almost a factor of two, suggesting that the discontinuity is real and not accidental. Unlike the well-known Parenago discontinuity, which results from the subdivision of stars into objects of the disk, intermediate component, and halo, this discontinuity is due to a subtler effect: stars of the thick and thin disks contribute differently to the determination of the kinematic parameters. At

$\tau \approx 9$ Gyr, the velocity lags (asymmetric drifts) of the thin and thick disks are V_ϕ=11 and V_ϕ=35 km/s, respectively.

The mean velocity component along the x coordinate averaged over all the stars remains constant, and equal to $X_{\odot\,\mathrm{LSR}} = 8.7 \pm 0.5$ km/s. Imposing constraints on $|V_{pec}|$ leads to the appearance of appreciable gradient of this quantity as a function of time, and this velocity reaches 3.0 ± 0.8 km/s for the oldest disk stars. The z velocity component for all the stars considered is the most stable, and is equal, on average, to $Z_{\odot\,\mathrm{LSR}} = 7.2 \pm 0.8$ km/s. Our extrapolation of the residual-velocity dispersion to zero yielded $Y_{\odot\,\mathrm{LSR}} = 6.2 \pm 2.2$ km/s.

ACKNOWLEDGMENTS

We thank the reviewer for valuable comments that improved the paper, and to R.B. Shatsova and G.B. Anisimova for calling our attention to the problem of the discontinuity of the Strömberg asymmetry. This work was supported by the Russian Foundation for Basic Research (project code 05-02-17047).

REFERENCES

1. K. Schwarzschild, Nachr. Königlichen Ges. Wiss. Göttingen, **191** (1908).

2. J. Skuljan, J. B. Hearnshaw, and P. L. Cottrell, MNRAS **308**, 731 (1999).

3. W. Dehnen, Astron. J. **115**, 2384 (1998).

4. E. Chereul, M. Crézé, and O. Bienaymé, Astron. Astrophys. **340**, 384 (1998).

5. E. Chereul , M. Crézé, and O. Bienaymé *et al.*, Astron. Astrophys. Suppl. Ser. **135**, 5 (1999).

6. R. Asiain, F. Figueras, J. Torra *et al.*, Astron. Astrophys. **341**, 427 (1999).

7. D. R. Soderblom, B. F. Jones, S. Balachandran *et al.*, Astron. J. **106**, 1059 (1993).

8. J. R. King, A. R. Villarreal, D. R. Soderblom *et al.*, Astron. J. **125**, 1980 (2003).

9. V. Castellani, S. Degl'Innocenti, and P. Moroni, MNRAS **320**, 66 (2001).

10. S. Chandrasekhar, *Principles of stellar dynamics* (Yerkes Observatory, 1942; IL, Moscow, 1948).

11. J. C. Kapteyn, British Assoc. Adv. Sci. Rep., 257 (1905).

12. O. J. Eggen, Astron. J. **111**, 1615 (1995).

13. O. J. Eggen, Astron. J. **112**, 1595 (1996).

14. ESA SP-1200, The Hipparcos and Tycho Catalogues (1997).

15. W. Dehnen and J. J. Binney, MNRAS **298**, 387 (1998).

16. B. Nordström, M. Mayor, J. Andersen *et al.*, Astron. Astrophys. **419**, 989 (2004).

17. B. Famaey, A. Jorissen, X. Luri *et al.*, Astron. Astrophys. **430**, 165 (2005).

18. E. Høg, C. Fabricius, V.V. Makarov *et al.*, Astron. Astrophys. **355**, L27 (2000).

19. V. V. Bobylev, Pis'ma Astron. Zh. **30**, 185 (2004) [Astron. Lett. **30**, 159 (2004)].

20. K. F. Ogorodnikov, Dynamics of Stellar Systems (Fizmatgiz, Moscow, 1958; Pergamon, Oxford, 1965).

21. P. P. Parenago, Kurs zvezdnoi astronomii (Course of Stellar Astronomy) (Gosizdat, Moscow, 1954) [in Russian].

22. R. J. Trumpler and H. F.Weaver, Statistical Astronomy (Univ. of Calif. Press, Berkely, 1953).

23. P. P. Parenago, Tr. Gos. Astron. Inst. im. P.K. Sternberga **20**, 26 (1951).

24. R. Olling and W. Dehnen, Astroph. J. **599**, 275 (2003).

25. I. R. King, *An Introduction to Classical Stellar Dynamics* (University of California, Berkeley, 1994; USSR, Moscow, 2002).

26. A. C. Robin, C. Reylé, S. Derrière *et al.*, Astron. Astrophys. **409**, 523 (2003).

27. A. E. Gómez, S. Grenier, S. Udry *et al.*, ESA SP-402: Hipparcos-Venice' 97, 402 (1997).

28. R. S. De Simone, X. Wu, and S. Tremaine, MNRAS **350**, 627 (2004).

29. R. Fux, Astron. Astrophys. **373**, 511 (2001).

30. G. Mühlbauer and W. Dehnen, Astron. Astrophys. **401**, 975 (2003).

31. C. Babusiaux and G. Gilmore, MNRAS **358**, 1309 (2005).

32. W. Dehnen, Astroph. J. **524**, L35 (1999).

33. W. Dehnen, Astron. J. **119**, 800 (2000).

34. L. S.Marochnik and A. A. Suchkov, Galaktika (The Galaxy) (Nauka, Moscow, 1984) [in Russian].

35. T. V. Borkova and V. A. Marsakov, Pis'ma Astron. Zh. **30**, 174 (2004) [Astron. Lett. **30**, 148 (2004)].

Translated by A. Dambis

Table 1. Parameters of the solar motion.

Sample	$N_\star$	$\overline{r}$, pc	$\overline{\tau}$, Gyr	$X_\odot$, km/s	$Y_\odot$, km/s	$Z_\odot$, km/s	$V_\odot$, km/s	$L_\odot$	$B_\odot$
t1	1205	107	1.5±0.3	11.6±0.5	14.6±0.5	7.0±0.5	19.9±0.5	$52^o \pm 2^o$	$21^o \pm 2^o$
t2	1281	96	2.5±0.5	9.4±0.6	15.2±0.6	7.4±0.6	19.3±0.6	58±2	22±2
t3	1304	80	4.3±1.3	7.9±0.7	15.5±0.7	7.8±0.7	19.1±0.7	63±2	24±2
t4	1214	69	8.9±2.5	8.6±0.9	25.2±0.9	6.8±0.9	27.5±0.9	71±2	14±2
t1′	1116	107	1.5±0.3	9.7±0.5	13.1±0.5	7.0±0.5	17.8±0.5	53±2	23±2
t2′	1130	95	2.5±0.5	7.2±0.5	13.8±0.6	6.9±0.5	17.0±0.5	62±2	24±2
t3′	968	78	4.2±1.3	5.1±0.6	13.7±0.6	6.7±0.6	16.0±0.6	70±2	25±2
t4′	731	67	8.6±2.5	3.0±0.8	16.0±0.8	5.7±0.8	17.2±0.8	79±3	19±3
t1″	71	112	1.6±0.3	45.9±2.7	34.7±2.7	8.7±2.7	58.2±2.7	37±3	9±3
t2″	102	103	2.5±0.5	36.7±2.8	33.9±2.8	12.2±2.8	51.4±2.8	43±3	14±3
t3″	186	81	4.5±1.3	18.9±2.6	33.1±2.6	12.3±2.6	40.0±2.6	60±4	18±4
t4″	294	68	9.3±2.5	16.6±2.2	39.8±2.2	9.6±2.2	44.1±2.2	67±3	13±3

$N_\star$ is the number of stars and r the heliocentric distance of the star.

Table 2. Parameters of the solar motion

	σ_1	σ_2	σ_3	$l_1,\ b_1$	$l_2,\ b_2$	$l_3,\ b_3$
t1	23.6±0.6	13.7±0.6	10.8±0.4	$15^o \pm 2^o,\ \ 1^o \pm 0^o$	$105^o \pm 2^o,\ -1^o \pm 1^o$	$127^o \pm 2^o,\ 89^o \pm 4^o$
t2	25.6±0.7	16.0±0.5	13.0±0.3	12±1, 0±0	102±2, 6±1	281±2, 85±4
t3	29.1±0.8	19.2±0.6	15.7±0.4	7±1, 0±0	97±2, 9±2	275±2, 81±6
t4	35.4±1.0	23.7±0.7	20.9±0.6	7±8, -1±1	97±3, 8±2	284±3, 82±8

Table 3. Normalized amplitudes of the main peaks in the UV velocity distribution

Sample	Hyades	Pleiades	Sirius	Coma
t1	48.20	8.62	13.88	5.84
t2	17.56	13.42	20.18	11.54
t3	30.30	11.57	11.59	4.31
t4	16.19	2.69	5.27	3.96

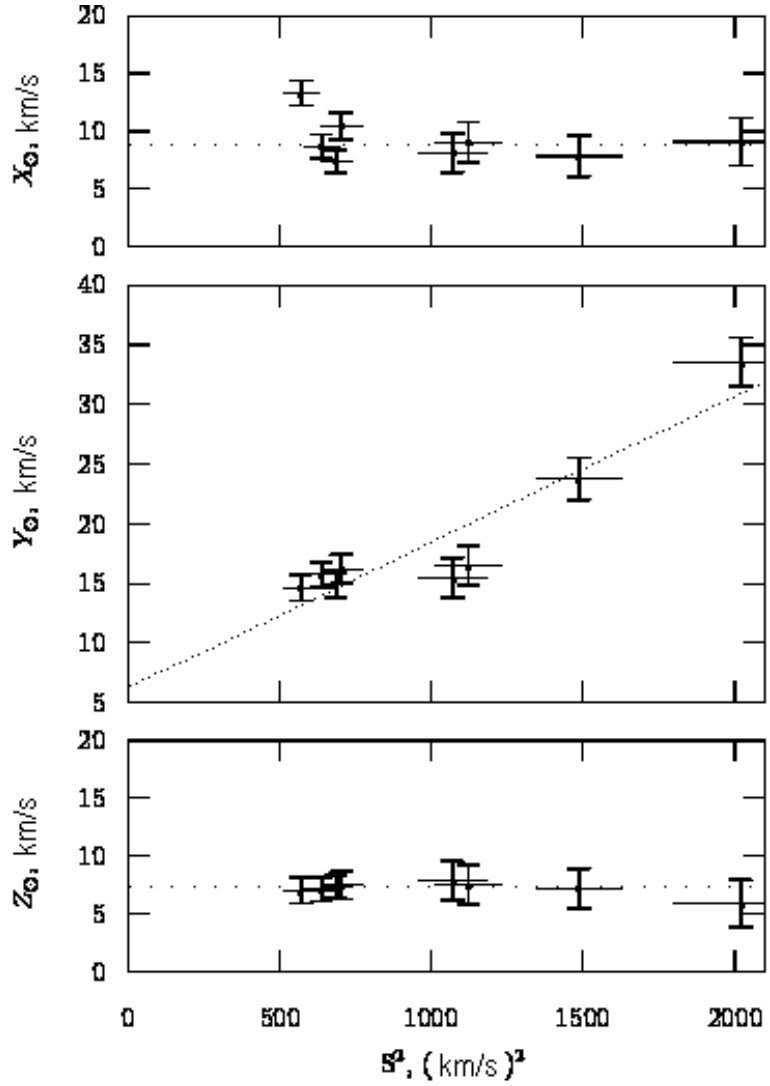

Fig. 1. Solar velocity components as a function of the square of the residual stellar-velocity dispersion.

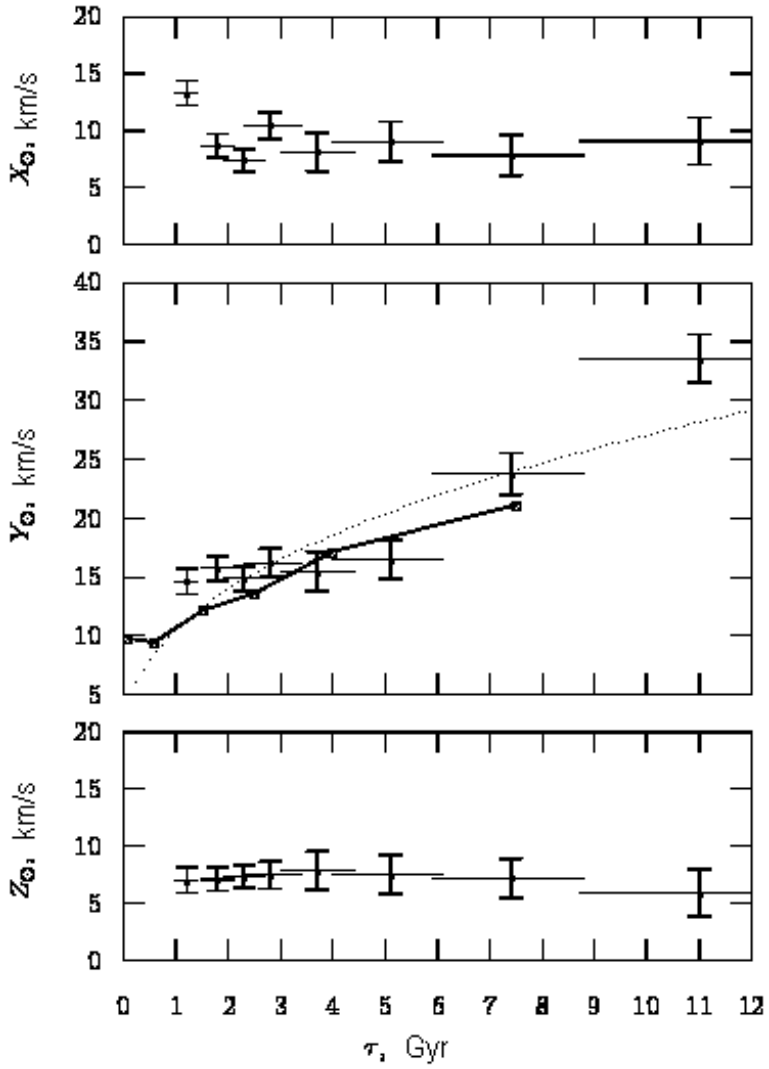

Fig. 2. Solar velocity components as a function of stellar age.

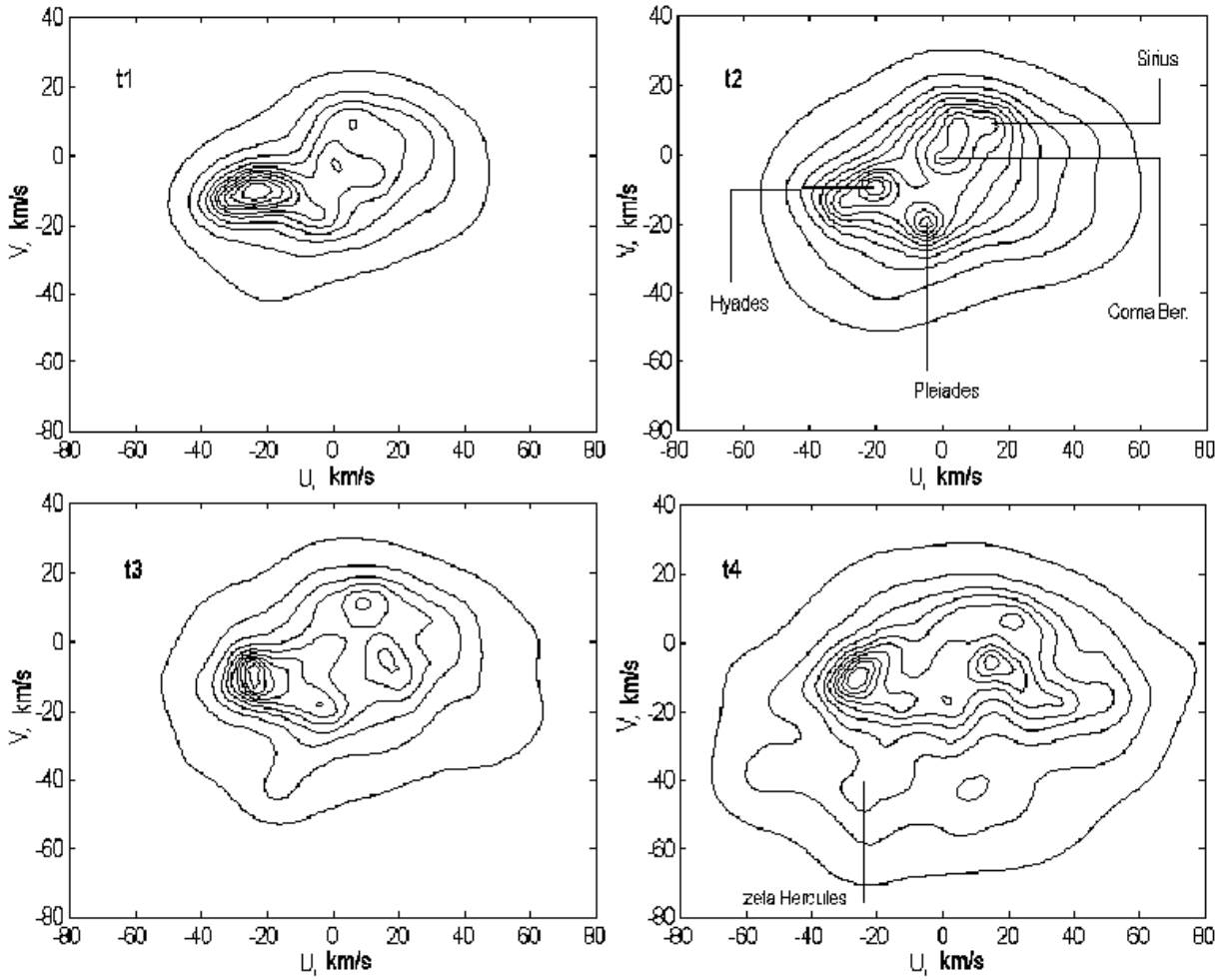

Fig. 3. Distributions of UV velocity components of the stars in four stellar age groups.

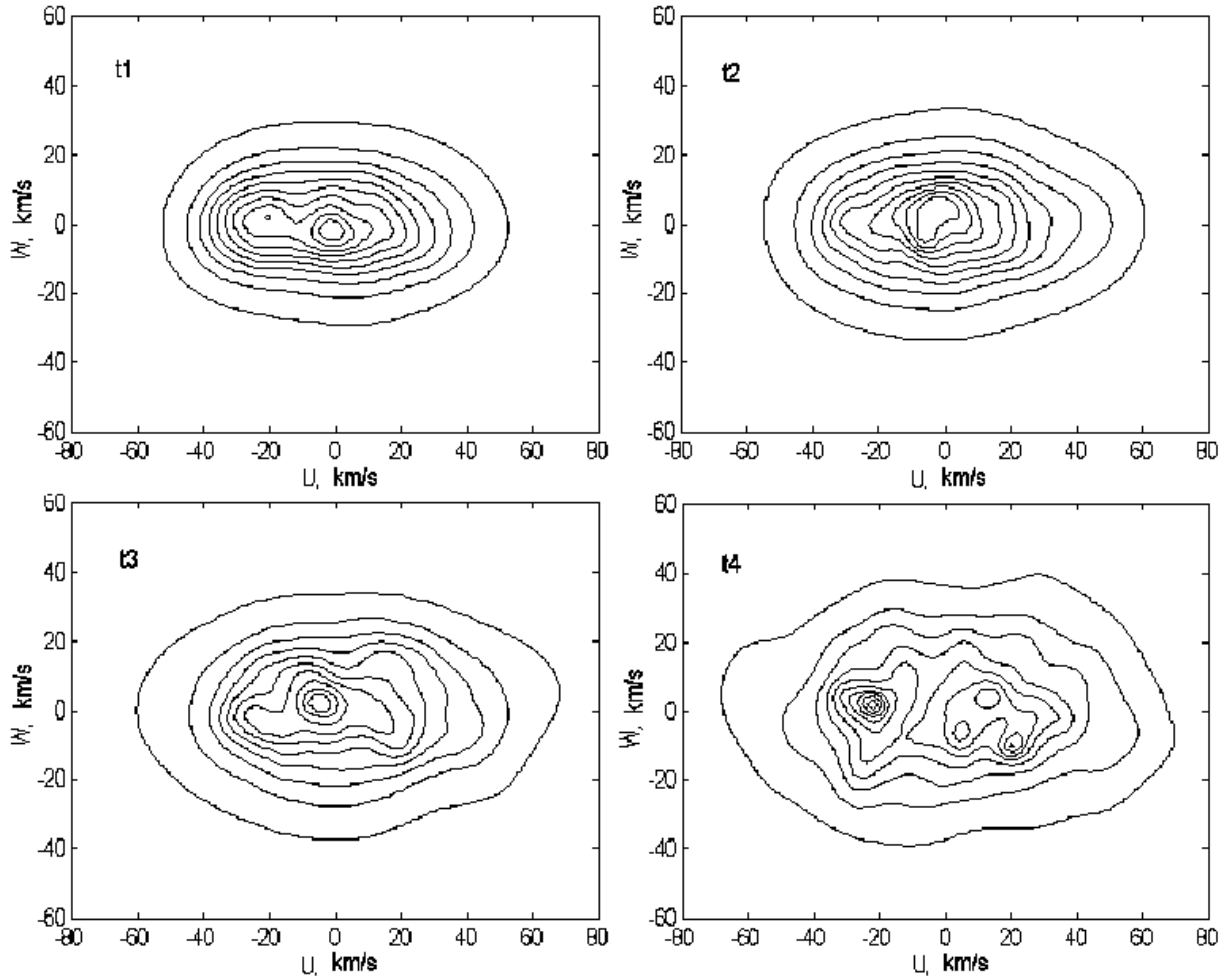

Fig. 4. Same as Fig. 3 for the UW velocity components of the stars.

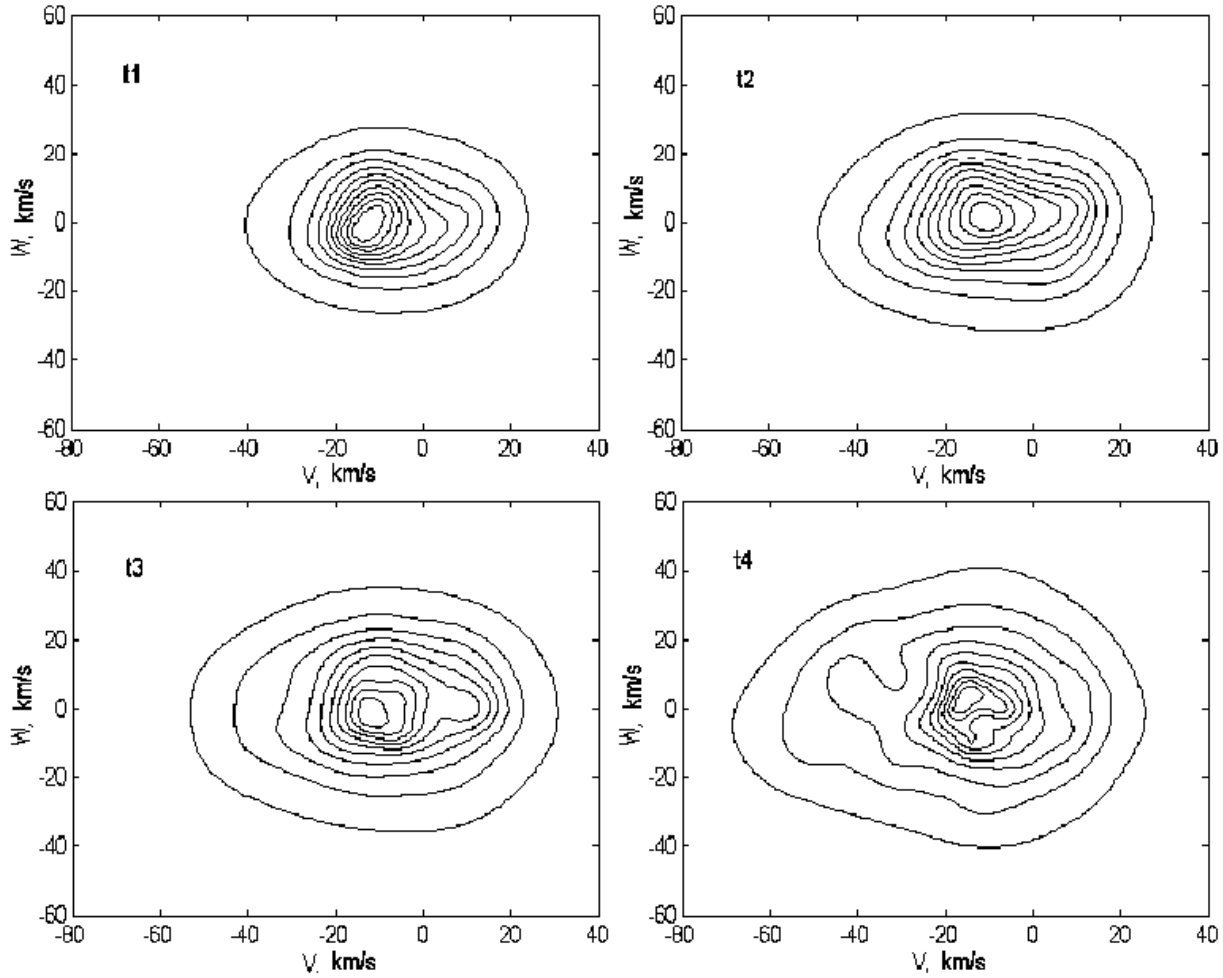

Fig. 5. Same as Fig. 3 for the VW velocity components of the stars.

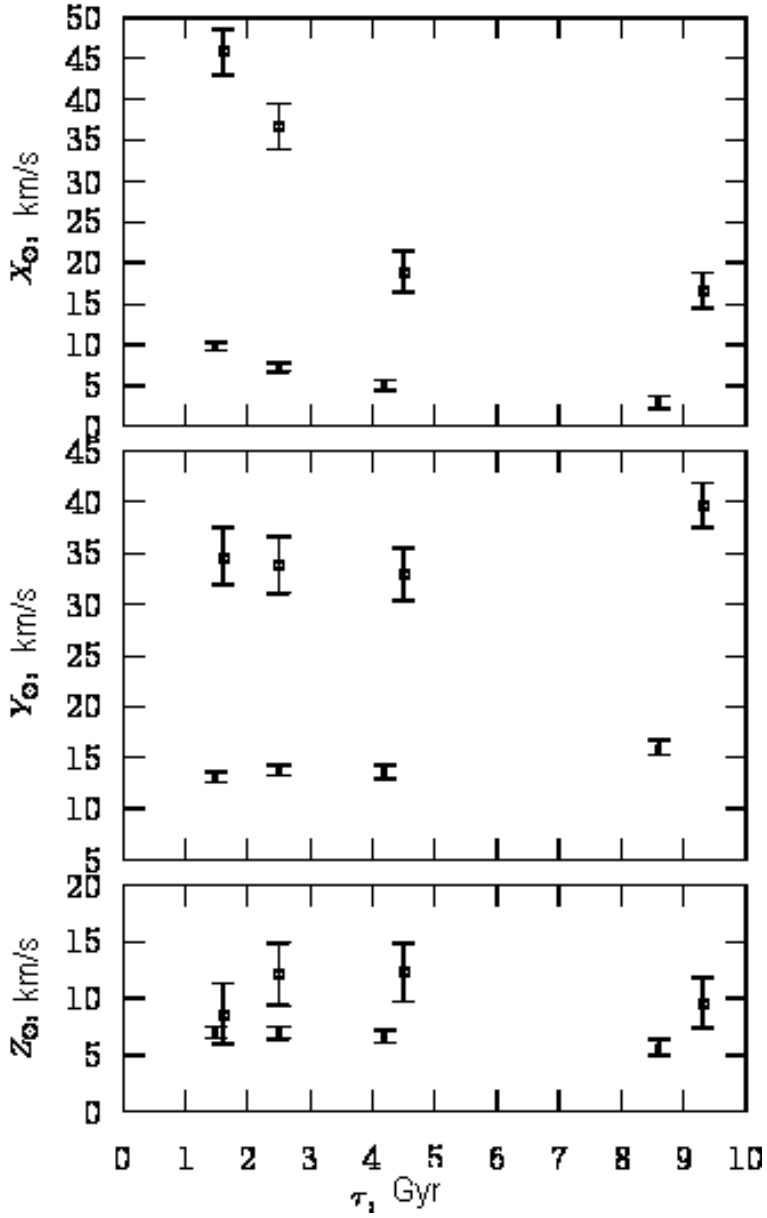

Fig. 6. Components of the solar velocity as a function of the age of stars belonging to the thin disk (filled squares) and thick disk (open circles).